
AdapterGNN: Efficient Delta Tuning Improves Generalization Ability in Graph Neural Networks

Shengrui Li^{1,2,*}, Xuetong Han^{2,†}, Jing Bai²

¹Tsinghua University, ²Microsoft Research Asia

1sr22@mails.tsinghua.edu.cn, chrihan@microsoft.com, jbai@microsoft.com

Abstract

Fine-tuning pre-trained models has recently yielded remarkable performance gains in graph neural networks (GNNs). In addition to pre-training techniques, inspired by the latest work in the natural language fields, more recent work has shifted towards applying effective fine-tuning approaches, such as parameter-efficient tuning (delta tuning). However, given the substantial differences between GNNs and transformer-based models, applying such approaches directly to GNNs proved to be less effective. In this paper, we present a comprehensive comparison of delta tuning techniques for GNNs and propose a novel delta tuning method specifically designed for GNNs, called AdapterGNN. AdapterGNN preserves the knowledge of the large pre-trained model and leverages highly expressive adapters for GNNs, which can adapt to downstream tasks effectively with only a few parameters, while also improving the model’s generalization ability on the downstream tasks. Extensive experiments show that AdapterGNN achieves higher evaluation performance (outperforming full fine-tuning by 1.4% and 5.5% in the chemistry and biology domains respectively, with only 5% of its parameters tuned) and lower generalization gaps compared to full fine-tuning. Moreover, we empirically show that a larger GNN model can have a worse generalization ability, which differs from the trend observed in large language models. We have also provided a theoretical justification for delta tuning can improve the generalization ability of GNNs by applying generalization bounds.

1 Introduction

Graph neural networks (GNNs) [29; 39] have achieved remarkable success in analyzing graph-structured data [11; 34; 42] but face challenges such as the scarcity of labeled data and low out-of-distribution generalization ability. To overcome these challenges, recent efforts have focused on designing GNNs pre-training approaches [17; 40; 43] that leverage abundant unlabeled data to capture transferable intrinsic graph properties and generalize them to different downstream tasks by fine-tuning [46; 47; 36]. While fine-tuning all parameters from a pre-trained model can improve performance [28; 17], it usually requires a relatively large model architecture to effectively glean knowledge from pre-training tasks [6; 4]. This becomes challenging when the downstream task has limited data, as optimizing a large number of parameters can lead to overfitting [20]. Moreover, training and maintaining a separate large-scale model for each task can prove to be inefficient as the number of tasks grows. To address these challenges, recent research has focused on developing parameter-efficient tuning (delta tuning) techniques that can effectively adapt pre-trained models to new tasks [8], such as adapter tuning [15], LoRA [16], BitFit [44], prefix-tuning [22], and the prompt tuning [21]. Delta tuning seeks to tune a small portion of parameters and keep the left parameters frozen. This approach reduces training costs and allows for use in low-data scenarios.

*Work is done during internship at Microsoft Research Asia. [†]Corresponding author.

Researchers have recently discovered that these techniques from natural language processing (NLP) could be applied to the GNNs field [41]. In particular, the idea of prompt tuning has been widely recognized, and many efforts have been made to adopt this technique to GNNs [38]. This adoption involves either manual prompt engineering [32] or soft prompt tuning techniques [24; 7; 9]. However, most of these methods tune all parameters of pre-trained GNNs to ensure comparable performance, while other delta tuning methods which freeze most parameters struggle to match the full fine-tuning baseline [9], unless in special few-shot setting [24]. They only explore prompt-based approaches in GNNs without comparing them to other delta tuning methods. Prompt-based methods involve modifying only the raw input and not the inner architecture. Furthermore, due to the intrinsic difference between transformer-based models and GNNs, not all NLP solutions can be directly applied to GNNs.

To address this issue, we conduct a comprehensive analysis of various delta tuning approaches in GNNs and propose an effective method, AdapterGNN, specifically designed to cater to the non-transformer GNN architecture with novel techniques. AdapterGNN combines task-specific knowledge in tunable adapters with task-agnostic knowledge in the frozen pre-trained model.

Delta tuning addresses two drawbacks of fine-tuning to improve generalization ability. The first drawback, **P1**, is the catastrophic forgetting of pre-trained knowledge, which is disastrous during generalizing [18]. Since delta tuning only tunes minimal parameters and keeps most parameters fixed, catastrophic forgetting can be potentially mitigated, resulting in improved model transferability and generalization [8]. The second drawback, **P2**, is overfitting when tuning on a small dataset with large parameters [1; 2], particularly in the OOD case [19; 17]. To mitigate overfitting and promote generalization ability, delta tuning reduces the size of the tunable parameter space. This is especially important in scenarios where the dataset is limited. We illustrate this in Fig. 1 and provide a detailed theoretical justification from the perspective of generalization bounds [25; 30] in Sec. 3.

Our improved performance can be attributed to our specially designed architecture that effectively utilizes the advantages of delta tuning while preserving the expressivity of GNNs.

To conclude, our work makes the following contributions:

- While previous work has mainly focused on applying prompt tuning to GNNs, we present a comprehensive comparison of delta tuning approaches and show that prompt tuning may not be the best fit for the field. We propose an effective delta tuning framework specifically designed for GNNs, called AdapterGNN. To the best of our knowledge, it is the first adapter variant with several novel techniques that work in GNNs and the first method outperforms full fine-tuning while keeping most parameters frozen.
- We provide a theoretical justification for how delta tuning improves the generalization ability to improve performance in GNNs from the perspective of generalization bounds.
- Extensive experiments demonstrate that with only 5% parameters tuned, our method surpasses full fine-tuning baselines by an average of 1.4% and 5.5% in two domains. It also outperforms other state-of-the-art delta tuning methods by a significant margin.

2 Related Work

Delta tuning methods. Full fine-tuning tunes all the model parameters and adapts them to downstream tasks, but this becomes inefficient with the growth of model size and task count. Recent NLP

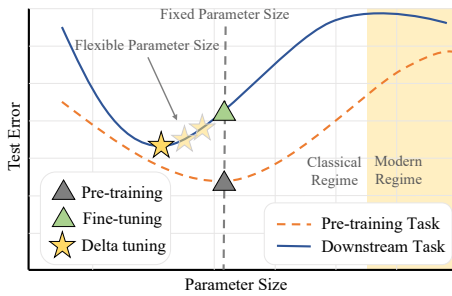


Figure 1: A large model is often employed for pre-training \blacktriangle when sufficient data is available. However, for downstream tasks with limited data, a smaller model is optimal in the classical regime. Compared with fine-tuning \blacktriangle , delta tuning \star preserves expressivity while reducing the size of parameter space, leading to lower test error.

work has explored delta tuning techniques that tune only a small portion of parameters for efficiency [8]. Prompt tuning [21] aims to modify model inputs rather than model architecture. Prefix-tuning [22] only updates task-specific trainable parameters in each layer. Adapter tuning [15; 5] inserts adapter modules with bottleneck architecture between layers. BitFit [44] only updates the bias terms while freezing the remaining. LoRA [16] decomposes the weight matrix into low-rank matrices to reduce the number of trainable parameters. As for the GNNs field, the idea of prompt tuning has gained widespread acceptance [38]. GPPT [32] specially designs a framework for GNNs but is limited to node-level tasks. Limited to the molecular field, MolCPT [7] encodes additional molecular motif information to enhance graph embedding. GPF [9] and GraphPrompt [24] are parameter-efficient but struggle to match the full fine-tuning baseline in the non-few-shot setting.

Generalization error bounds. Generalization error bounds, also known as generalization bounds, provide insights into the predictive performance of learning algorithms in statistical machine learning. In the classical regime, bias-variance tradeoff states that the test error as a function of model complexity follows the U-shaped behavior [25; 30]. However, in the over-parameterized regime, increasing complexity decreases test error, following the modern intuition of "larger model generalizes better" [3; 27; 45; 33; 13; 26]. [1] has theoretically analyzed generalization on over-parameterized large language models, it explains the empirical results that larger pre-trained models generalize better by applying compression-based generalization bounds. While our work utilizes conventional generalization bounds to analyze the generalization ability of delta tuning on GNNs.

3 Delta Tuning Improving Generalization Ability in GNNs

In this section, we theoretically demonstrate delta tuning can lower the bounds of test error (generalization bounds) and improve generalization ability in GNNs compared to full fine-tuning.

Our empirical findings in Appendix C.1 show that our tasks exhibit a phenomenon where performance gets worse as we increase model size. Hence, we apply a widely used generalization bounds theorem [1; 2] and the detailed proof of this theorem can be found in Appendix B.1:

Theorem 1 *Generalization bounds for finite hypothesis space in classical regime.* *Training data \mathcal{D}_n and the trained parameters \mathcal{P} are variables of training error $\hat{\mathcal{E}}$. The number of training samples n and size of parameter space $|\mathcal{P}|$ are variables of generalization gap bounds. Then, statistically, the upper bound $\mathcal{U}(\mathcal{E})$ of the test error \mathcal{E} of a model in finite hypothesis space is determined as follows:*

$$\mathcal{E} \leq \mathcal{U}(\mathcal{E}) = \hat{\mathcal{E}}(\mathcal{D}_n, \mathcal{P}) + O\left(\sqrt{|\mathcal{P}|/n}\right). \quad (1)$$

Before introducing delta tuning, we first compare the error bounds of two paradigms: "supervised training from scratch" and "pre-train, fine-tune". For supervised training from scratch, we denote the task as T and training data as $\mathcal{D}_{n_T}^T$. With the increase of $|\mathcal{P}_T|$, training error $\hat{\mathcal{E}}(\mathcal{D}_{n_T}^T, \mathcal{P}_T)$ decreases due to stronger optimization capability and generalization gap bounds $O(\sqrt{|\mathcal{P}_T|/n_T})$ increases. Therefore, following the U-shaped behavior, the following corollary is obtained and the detailed proof can be found in Appendix B.2:

Corollary 1 *Bounds of supervised training from scratch.* *There is an optimal $|\mathcal{P}_T|$ to get the tightest upper bound $\min(\mathcal{U}(\mathcal{E}_T)) = \hat{\mathcal{E}}(\mathcal{D}_{n_T}^T, \bar{\mathcal{P}}_T) + O\left(\sqrt{|\bar{\mathcal{P}}_T|/n_T}\right)$.*

For pre-training task S , data is more abundant: $n_S > n_T$. Many previous works discover that with abundant data to pre-train, we should employ a larger model to capture sufficient knowledge [12; 8; 37]. Therefore, we have the following corollary and the proof can be found in Appendix B.3:

Corollary 2 *Bounds of pre-training.* *For the pre-training task S satisfying $n_S > n_T$, there is also an optimal $|\bar{\mathcal{P}}_S|$ and $|\bar{\mathcal{P}}_S| > |\bar{\mathcal{P}}_T|$ to get the tightest upper bound $\min(\mathcal{U}(\mathcal{E}_S)) = \hat{\mathcal{E}}(\mathcal{D}_{n_S}^S, \bar{\mathcal{P}}_S) + O\left(\sqrt{|\bar{\mathcal{P}}_S|/n_S}\right)$.*

In the "pre-train, fine-tune" paradigm, a model that has been pre-trained on task S is used as initialization to improve the performance of a supervised task. To account for the effect of the initial parameter values, we use $\hat{\mathcal{E}}_S(D, \mathcal{P})$ to denote the training error of the pre-trained model.

Compared to training from scratch with the same model as pre-training: $\mathcal{U}(\mathcal{E}_T) = \hat{\mathcal{E}}(\mathcal{D}_{n_T}^T, \bar{\mathcal{P}}_S) + O\left(\sqrt{|\bar{\mathcal{P}}_S|/n_T}\right)$, fine-tuning benefits from a better initialization, which leads to a lower error bound: $\mathcal{U}(\mathcal{E}_F) = \hat{\mathcal{E}}_S(\mathcal{D}_{n_T}^T, \bar{\mathcal{P}}_S) + O\left(\sqrt{|\bar{\mathcal{P}}_S|/n_T}\right)$. Based on this, we make the following assumption and corollary:

Assumption 1 *The Transfer Gain \mathbf{TG} from the pre-trained model can be quantified. It is solely determined by the properties of S, T and can be calculated as: $\mathbf{TG} = \hat{\mathcal{E}}(\mathcal{D}_{n_T}^T, \bar{\mathcal{P}}_S) - \hat{\mathcal{E}}_S(\mathcal{D}_{n_T}^T, \bar{\mathcal{P}}_S)$*

Corollary 3 Bounds of fine-tuning. *Fine-tuning a pre-trained model can result in a lower error bound, which can be measured by the transfer gain denoted by \mathbf{TG} :*

$$\mathcal{U}(\mathcal{E}_F) = \hat{\mathcal{E}}(\mathcal{D}_{n_T}^T, \bar{\mathcal{P}}_S) + O\left(\sqrt{|\bar{\mathcal{P}}_S|/n_T}\right) - \mathbf{TG} \quad (2)$$

In regard to delta tuning, the delta tuning model is initialized with the same pre-trained parameters as fine-tuning, so \mathbf{TG} is inherited similarly to fine-tuning, leading to the following corollary:

Corollary 4 Bounds of delta tuning. *Bounds of delta tuning share a similar form as fine-tuning:*

$$\mathcal{U}(\mathcal{E}_D) = \hat{\mathcal{E}}(\mathcal{D}_{n_T}^T, \mathcal{P}_D) + O\left(\sqrt{|\mathcal{P}_D|/n_T}\right) - \mathbf{TG}. \quad (3)$$

For delta tuning, we propose a prerequisite: the preservation of the expressivity of full fine-tuning GNNs. Our AdapterGNN is specifically designed to maximally maintain the capacity of the original GNNs. So, it can be almost as powerful as full fine-tuning with much smaller parameters. In contrast, several delta tuning techniques have failed to yield satisfactory results in GNNs, such as prompt tuning [9; 24]. This can be attributed to not meeting this prerequisite.

With this prerequisite, when training from scratch on T , the trainable structure of delta tuning and fine-tuning yields similar minimal generalization errors (under $\bar{\mathcal{P}}_T$ and $\bar{\mathcal{P}}_D$, respectively) as follows:

$$\left| \left(\hat{\mathcal{E}}(\mathcal{D}_{n_T}^T, \bar{\mathcal{P}}_T) + O\left(\sqrt{|\bar{\mathcal{P}}_T|/n_T}\right) \right) - \left(\hat{\mathcal{E}}(\mathcal{D}_{n_T}^T, \bar{\mathcal{P}}_D) + O\left(\sqrt{|\bar{\mathcal{P}}_D|/n_T}\right) \right) \right| < \varepsilon. \quad (4)$$

And for downstream task T , the optimal size is $|\bar{\mathcal{P}}_T|$ as in Cor. 1. But Cor. 2 gives $|\bar{\mathcal{P}}_S| > |\bar{\mathcal{P}}_T|$. Therefore, error bound $\mathcal{U}(\mathcal{E}_T)$ under $|\bar{\mathcal{P}}_S|$ is larger than that under the optimal $|\bar{\mathcal{P}}_T|$:

$$\min(\mathcal{U}(\mathcal{E}_T)) = \hat{\mathcal{E}}(\mathcal{D}_{n_T}^T, \bar{\mathcal{P}}_T) + O\left(\sqrt{|\bar{\mathcal{P}}_T|/n_T}\right) < \hat{\mathcal{E}}(\mathcal{D}_{n_T}^T, \bar{\mathcal{P}}_S) + O\left(\sqrt{|\bar{\mathcal{P}}_S|/n_T}\right) \quad (5)$$

This means reducing the size of parameter size leads to a decrease in test error, which is aligned with the phenomena in the classical regime. We also empirically validate this trend in Appendix C.1. We define this **Reduction Gain** as: $\mathbf{RG} = \hat{\mathcal{E}}(\mathcal{D}_{n_T}^T, \bar{\mathcal{P}}_S) + O\left(\sqrt{|\bar{\mathcal{P}}_S|/n_T}\right) - \left(\hat{\mathcal{E}}(\mathcal{D}_{n_T}^T, \bar{\mathcal{P}}_T) + O\left(\sqrt{|\bar{\mathcal{P}}_T|/n_T}\right) \right)$.

Combining Equation 2,3, Inequality 4, and definition of **RG**, we obtain the following proposition:

Proposition 1 Conditioned on $\varepsilon < \mathbf{RG}$, delta tuning has tighter bounds than fine-tuning. *Compare the tightest upper bound of delta tuning on $|\mathcal{P}_D|$ (where $|\mathcal{P}_D| < |\bar{\mathcal{P}}_S|$) with the bounds of fine-tuning:*

$$\begin{aligned} & \mathcal{U}(\mathcal{E}_F) - \min(\mathcal{U}(\mathcal{E}_D)) \\ &= \hat{\mathcal{E}}(\mathcal{D}_{n_T}^T, \bar{\mathcal{P}}_S) + O\left(\sqrt{|\bar{\mathcal{P}}_S|/n_T}\right) - \mathbf{TG} - \left(\hat{\mathcal{E}}(\mathcal{D}_{n_T}^T, \bar{\mathcal{P}}_D) + O\left(\sqrt{|\bar{\mathcal{P}}_D|/n_T}\right) - \mathbf{TG} \right) \\ &> \hat{\mathcal{E}}(\mathcal{D}_{n_T}^T, \bar{\mathcal{P}}_S) + O\left(\sqrt{|\bar{\mathcal{P}}_S|/n_T}\right) - \left(\hat{\mathcal{E}}(\mathcal{D}_{n_T}^T, \bar{\mathcal{P}}_T) + O\left(\sqrt{|\bar{\mathcal{P}}_T|/n_T}\right) \right) - \varepsilon = \mathbf{RG} - \varepsilon \end{aligned} \quad (6)$$

If delta tuning preserves enough expressivity and **RG** is large enough, the condition $\varepsilon < \mathbf{RG}$ is satisfied. Therefore, delta tuning provides tighter bounds than fine-tuning.

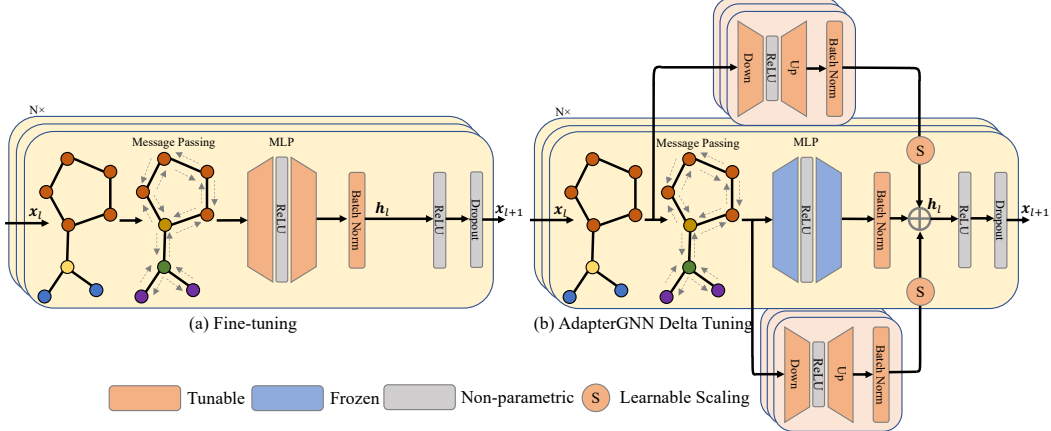


Figure 2: **Comparison between full fine-tuning and AdapterGNN delta tuning on GIN.** a) The full fine-tuning updates all parameters of each pre-trained GNN layer. (b) AdapterGNN includes two parallel adapters taking input before and after the message passing. Their outputs are added to the original output of batch normalization with learnable scaling. During tuning, the original MLP of each GNN layer, which comprises the majority of the parameters, is frozen.

4 Methodology

4.1 AdapterGNN

We propose a delta tuning framework called AdapterGNN. AdapterGNN utilizes ideas adopted in adapters [15] as well as several novel techniques specially designed for GNNs. The framework is demonstrated in Fig. 2. It adds trainable adapters in parallel to GNN MLPs, combining task-specific knowledge in adapters with task-agnostic knowledge from the pre-trained model. We will introduce the key techniques as follows.

Architecture. As mentioned in Sec. 3, preserving the expressivity of the full fine-tuning GNNs is crucial for delta tuning to generalize better than full fine-tuning. To enhance expressivity, we utilize the below techniques. The multi-layer perception (MLP) module contains the majority of the learnable parameters and is important for GNNs. Therefore, we introduce adapters as parallel computations to the GNN MLPs. In each GNN layer, message passing (MP) aggregates information from the neighborhood. Node embeddings before and after MP provides complementary and informative information. To capture as much information as possible, we adopt two adapters, one taking input before MP and the other after. Additionally, data distribution may shift during tuning. It is essential to ensure that affine parameters in batch normalization (BN) are tunable during training. Also, to maintain consistency with the original output, we include tunable batch normalization in each adapter.

Adapter with bottleneck dimension. Adapter module utilize bottleneck architecture which includes a down-projection $\mathbf{W}_{\text{down}} : \mathbb{R}^{n_{\text{in}}} \rightarrow \mathbb{R}^{n_{\text{mid}}}$, a ReLU activation, and an up-projection $\mathbf{W}_{\text{up}} : \mathbb{R}^{n_{\text{mid}}} \rightarrow \mathbb{R}^{n_{\text{out}}}$. Unlike the original GNN MLP, the middle dimension n_{mid} is greatly reduced (e.g., $20\times$) as a bottleneck, resulting in a significant reduction in the size of tunable parameters space. With a BN attached, the output of the adapter is calculated as:

$$\mathbf{A}(\mathbf{x}) = \text{BN}(\mathbf{W}_{\text{up}}(\text{ReLU}(\mathbf{W}_{\text{down}}(\mathbf{x}))). \quad (7)$$

Learnable scaling to fuse output. The output of adapters and the original embedding are combined by element-wise addition:

$$\mathbf{h}_l = \text{BN}(\text{MLP}(\text{MP}(\mathbf{x}_l))) + s_1 \cdot \mathbf{A}_1(\mathbf{x}_l) + s_2 \cdot \mathbf{A}_2(\text{MP}(\mathbf{x}_l)). \quad (8)$$

where \mathbf{x}_l is the input of the l th layer and \mathbf{h}_l is the embedding before GNN ReLU and Dropout, i.e., $\mathbf{x}_{l+1} = \text{Dropout}(\text{ReLU}(\mathbf{h}_l))$. Previous work has either fixed s as 1 [15] or treated it as a hyperparameter [16; 5]. However, catastrophic forgetting may occur if s is large, and hyperparameter tuning can be time-consuming, which can significantly reduce the efficiency of delta tuning. Therefore,

Table 1: Comparison of different delta tuning techniques in GNNs. Average test ROC-AUC(%) and the proportion of tunable parameters(%) are reported. “-” represents the frozen baseline.

-	BitFit [44]	(IA) ³ [23]	LoRA [16]	Prompt feat	Prompt node	Adapter[15] seq	Adapter[15] par	Partial 1	Partial 3	Full	(ours)
Avg.	63.9	66.1	67.8	68.8	66.3	65.9	70.2	70.4	69.0	70.1	69.6
Param.	0.16	0.40	0.24	12.9	0.17	0.18	5.0	5.0	19.7	58.9	100
											71.2
											5.2

we propose using a learnable s , which we train from a very small starting point to avoid such issues. Our experiments demonstrate that this strategy can achieve stable and superior performance.

Initialize \mathbf{W}_{up} with zeros. We initialize the weights and bias of \mathbf{W}_{up} as zeros. Thus at the start of tuning, $\mathbf{A}(\mathbf{x}_l) = 0$, and \mathbf{h}_l is the same as the pre-trained model’s original \mathbf{h}_l . Along with a small starting scaling parameter s , we can enable the model to gradually acquire task-specific knowledge to prevent catastrophic forgetting.

4.2 Discussion

Effectiveness. Our framework provides several advantages. Firstly, **P1**: the issue of catastrophic forgetting of pre-trained knowledge, is effectively mitigated through our parallel adapter design and novel learnable scaling strategy. This strategy automatically controls the proportion of newly-tuned task-specific knowledge, while persistently preserving the pre-trained knowledge. Secondly, to address **P2**: overfitting when tuning on a small dataset with large parameters. Our framework introduces a bottleneck that significantly reduces the size of tunable parameter space. Sec. 3 has proved the reduction of parameter space size could alleviate overfitting and improve generalization, while also being highly efficient. Additionally, AdapterGNN is specifically designed for GNNs and takes input both before and after message passing. This strategy preserves expressivity as much as possible to satisfy the prerequisite to fully exploit the benefits of delta tuning.

Advantages over other delta tuning approaches. Delta tuning approaches for GNNs have not yet been widely employed. To bridge this gap, we present a comprehensive comparison of these techniques in Table 1. We evaluate the average ROC-AUC over six relatively small molecular datasets using an AttrMasking pre-trained model. Affine parameters for batch normalization are tunable for all techniques, including the frozen baseline.

Among the compared techniques, adapter-based methods are both efficient and effective. Our AdapterGNN inherits the advantages of the adapter and is specifically designed for GNNs, making it the best among all. This can be attributed to its superior expressivity, which is achieved through our novel design. On the other hand, BitFit only modifies the original bias, (IA)³ and LoRA only modify the output of linear layers, and prompt tuning only modifies the input. These techniques are less expressive and achieve inferior performance. Additionally, partially tuning GNN layers is less efficient. Detailed implementations of these techniques in GNNs can be found in Appendix D.2.

Applicability. Although our architecture is specifically designed for GIN [42], which is a powerful and widely used GNN model and can achieve state-of-the-art performance in our datasets. The design concept of AdapterGNN can be transferred to any existing GNN architecture such as GAT [34] and GraphSAGE [11]. This can be explored in future work.

5 Experiments

Experimental setup. We evaluate the effectiveness of AdapterGNN by conducting extensive graph-level classification experiments on eight molecular datasets and one biology dataset. We employ six different pre-training methods, all based on a GIN backbone. Details of datasets and pre-trained models are in Appendix D.3 and D.4. Implementations can be found in Appendix D.1.

Baseline methods. There are several state-of-the-art tuning methods in GNNs. GPPT [32] is specially designed for node classification but is difficult to extend to other tasks and is not parameter-efficient. GraphPrompt [24], modifies the output only, making it less expressive and only applicable

Table 2: Test ROC-AUC (%) performances on molecular prediction benchmarks with different tuning methods and pre-trained GNN models. "-" represents no pre-train.

Tuning Method	Pre-training Method	Dataset								Avg.
		BACE	BBBP	ClinTox	HIV	SIDER	Tox21	MUV	ToxCast	
Full Fine-tune (100%)	-	70.0 \pm 6.9	67.4 \pm 2.0	58.5 \pm 3.7	76.3 \pm 2.2	58.2 \pm 2.1	74.1 \pm 0.5	73.2 \pm 2.8	62.9 \pm 1.0	67.6
	Infomax	75.9 \pm 1.6	68.8 \pm 0.8	69.9 \pm 3.0	76.0 \pm 0.7	58.4 \pm 0.8	75.3 \pm 0.5	75.3 \pm 2.5	62.7 \pm 0.4	70.3
	EdgePred	79.9 \pm 0.9	67.3 \pm 2.4	64.1 \pm 3.7	76.3 \pm 1.0	60.4 \pm 0.7	76.0 \pm 0.6	74.1 \pm 2.1	64.1 \pm 0.6	70.3
	ContextPred	79.6 \pm 1.2	68.0 \pm 2.0	65.9 \pm 3.8	77.3 \pm 1.0	60.9 \pm 0.6	75.7 \pm 0.7	75.8 \pm 1.7	63.9 \pm 0.6	70.9
	AttrMasking	79.3 \pm 1.6	64.3 \pm 2.8	71.8 \pm 4.1	77.2 \pm 1.1	61.0 \pm 0.7	76.7 \pm 0.4	74.7 \pm 1.4	64.2 \pm 0.5	71.1
	GraphCL	74.6 \pm 2.2	68.6 \pm 2.3	69.8 \pm 7.2	78.5 \pm 1.2	59.6 \pm 0.7	74.4 \pm 0.5	73.7 \pm 2.7	62.9 \pm 0.4	70.3
	SimGRACE	74.7 \pm 1.0	69.0 \pm 1.0	59.9 \pm 2.3	74.6 \pm 1.2	59.1 \pm 0.6	73.9 \pm 0.4	71.0 \pm 1.9	61.8 \pm 0.4	68.0
AdapterGNN (ours) (5.2%)	Avg.	77.3	67.7	66.9	76.7	59.9	75.3	74.1	63.3	70.1
	-	73.4 \pm 2.4	66.4 \pm 1.4	57.9 \pm 3.5	76.8 \pm 1.3	59.3 \pm 0.7	74.8 \pm 0.7	74.8 \pm 1.6	63.9 \pm 0.5	68.4
	Infomax	75.1 \pm 1.9	67.0 \pm 1.6	69.2 \pm 2.8	77.6 \pm 1.0	58.9 \pm 1.1	75.6 \pm 0.7	76.8 \pm 1.9	62.9 \pm 0.5	70.4
	EdgePred	79.0 \pm 1.5	69.7 \pm 1.4	67.7 \pm 3.0	76.4 \pm 0.7	61.2 \pm 0.9	75.9 \pm 0.9	75.8 \pm 2.1	64.2 \pm 0.5	71.2
	ContextPred	78.7 \pm 2.0	68.2 \pm 2.9	68.7 \pm 5.3	76.1 \pm 0.5	61.1 \pm 1.0	75.4 \pm 0.6	76.3 \pm 1.0	63.2 \pm 0.3	71.0
	AttrMasking	79.7 \pm 1.3	67.5 \pm 2.2	78.3 \pm 2.6	76.7 \pm 1.2	61.3 \pm 1.1	76.6 \pm 0.5	78.4 \pm 0.7	63.6 \pm 0.5	72.8
	GraphCL	76.1 \pm 2.2	67.8 \pm 1.4	72.0 \pm 3.8	77.8 \pm 1.3	59.6 \pm 1.3	74.9 \pm 0.9	75.1 \pm 2.1	63.1 \pm 0.4	70.7
GPF[9] (0.1%)	SimGRACE	77.7 \pm 1.7	68.1 \pm 1.3	73.9 \pm 7.0	75.1 \pm 1.2	58.9 \pm 0.9	74.4 \pm 0.6	71.8 \pm 1.4	62.6 \pm 0.6	70.3
	Avg.	77.7	68.0	71.0	76.6	60.2	75.5	75.7	63.3	71.1
	Infomax	66.0 \pm 0.4	60.9 \pm 0.7	61.6 \pm 0.5	71.9 \pm 0.3	58.1 \pm 0.3	67.8 \pm 0.6	75.4 \pm 0.3	58.8 \pm 0.2	65.0
	EdgePred	68.0 \pm 0.4	55.9 \pm 0.2	50.8 \pm 0.1	66.0 \pm 0.7	51.5 \pm 0.7	63.1 \pm 0.5	63.1 \pm 0.1	55.7 \pm 0.5	59.3
	ContextPred	58.7 \pm 0.6	58.6 \pm 0.6	39.8 \pm 0.8	68.0 \pm 0.4	59.4 \pm 0.2	67.8 \pm 0.9	71.8 \pm 0.8	58.8 \pm 0.5	60.4
MolCPT[7] (40%)	AttrMasking	61.7 \pm 0.3	54.3 \pm 0.3	56.4 \pm 0.2	64.0 \pm 0.2	52.0 \pm 0.2	69.2 \pm 0.3	62.9 \pm 0.9	58.1 \pm 0.3	59.8
	GraphCL	71.5 \pm 0.6	63.7 \pm 0.4	64.5 \pm 0.6	70.3 \pm 0.5	55.3 \pm 0.6	65.5 \pm 0.5	70.1 \pm 0.7	58.5 \pm 0.5	64.9

Table 3: Test ROC-AUC (%) performances on PPI benchmark with different tuning methods and pre-trained GNN models.

Tuning Method	-	Infomax	EdgePred	ContextPred	AttrMasking	GraphCL	SimGRACE	Avg.
Full Fine-tune	65.2 \pm 1.2	64.0 \pm 1.2	65.6 \pm 0.9	63.5 \pm 1.1	63.2 \pm 1.2	65.5 \pm 0.8	68.2 \pm 1.2	65.0
AdapterGNN	66.3 \pm 0.9	67.4 \pm 1.5	70.6 \pm 1.1	67.2 \pm 1.5	68.2 \pm 1.4	68.1 \pm 1.5	70.1 \pm 1.2	68.6
GPF	65.9 \pm 1.9	62.9 \pm 1.0	51.2 \pm 1.3	67.1 \pm 0.6	69.0 \pm 0.3	62.3 \pm 0.5	50.0 \pm 0.9	60.4

in few-shot settings. GPF [9] on the other hand, only modifies the input by adding a prompt feature to the input embeddings. MolCPT [7] leverages molecular motifs to provide additional information to graph embedding. We compare AdapterGNN with GPF and MolCPT (with the GNN backbone frozen for fairness in efficiency) in our experiments.

5.1 Main Results

We compare AdapterGNN with full fine-tuning and other delta tuning methods on multiple pre-training methods and datasets, and **bold** the higher one. The results presented in Table 2 and Table 3 suggests the following observations:

(1) AdapterGNN generally outperforms full fine-tuning with much less tunable parameters. On molecular benchmarks, among eight datasets with six pre-training methods, AdapterGNN achieves higher/lower/equal performance than full fine-tuning in 30/17/1 cases for all experiments, 7/1/0 for average in datasets, and 6/0/0 for average in pre-training methods. The overall average ROC-AUC is 71.1%, which is 1.4% relatively higher. On the PPI benchmark, AdapterGNN achieves consistent superior performance. The overall average ROC-AUC is 68.6%, which is 5.5% higher. These improvements are achieved with only 5.2% tunable parameters.

(2) AdapterGNN outperforms state-of-the-art delta tuning methods by a large margin. Although GPF has a parameter efficiency of only 0.1%, its performance is limited. On molecular benchmarks, AdapterGNN has demonstrated significant improvements across five pre-training methods, with average improvements of 8.3%, 20.1%, 17.5%, 21.7%, and 8.9%, respectively. MolCPT with a fixed GNN backbone is also compared. Despite having frozen GNNs, MolCPT still has 40% tunable parameters. However, in comparison, AdapterGNN is able to outperform it by an average of 8.9% in GraphCL. On the PPI benchmark, compared with GPF, AdapterGNN is superior in 5 out of 6 pre-trained models and much more stable, outperforming it by an average of 13.6%.

(3) AdapterGNN avoids negative transfer and retains the stable improvements of pre-training. On the molecular benchmarks, pre-trained models outperform no pre-train by a significant margin in both full fine-tuning and AdapterGNN. However, on the PPI benchmark, negative transfer frequently occurs in full fine-tuning and GPF. But the benefits of pre-training remain stable in AdapterGNN.

5.2 Ablation Studies

First, we perform ablation studies on model size and training data size to validate our theoretical justification for the generalization bounds. Next, we investigate the properties that make for a good AdapterGNN. Specifically, we compare performance across different bottleneck dimensions, insertion forms, and scaling strategies. All models in the ablation study are pre-trained by AttrMasking. Unless otherwise specified, the performance represents the average ROC-AUC over six small molecular datasets, which is a representative and efficient criterion.

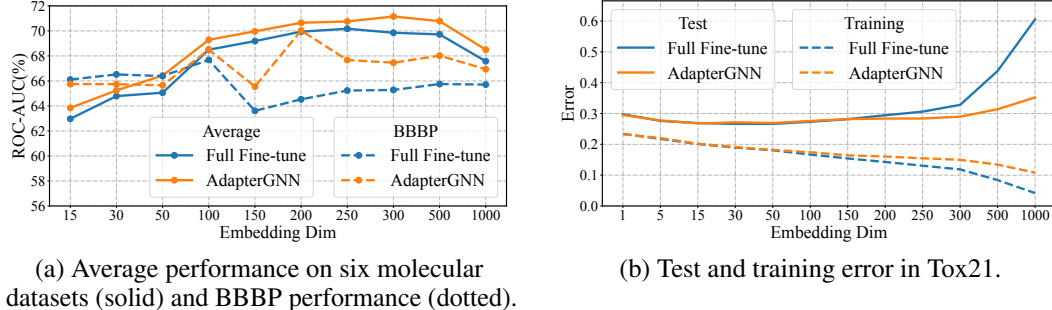


Figure 3: Test ROC-AUC (%) performances & errors with different model sizes.

Model size. We report performances and errors across model sizes by varying embedding dimensions. As shown in Fig. 3(a), average performances both initially increase and then decrease, indicating a larger model can be worse, which is consistent with the classical regime. AdapterGNN consistently outperforms full fine-tuning across all model sizes. Specifically, in the BBBP dataset, AdapterGNN may not surpass full fine-tuning with small model sizes, but it achieves superior performance in larger models. Fig. 3(b) displays the errors in the Tox21 dataset. The U-shaped test curve also validates the classical regime in our tasks. Although increasing the model size leads to a significant increase in the generalization gap (training error – test error) in full fine-tuning, the gap is well-controlled with AdapterGNN. This finding demonstrates AdapterGNN’s superior generalization ability, especially in larger models. Additionally, by comparing the optimal embedding dimension between models with and without pre-training from Fig. 3(a) with Fig. 6, it verifies the validity of $|\mathcal{P}_S| > |\mathcal{P}_T|$ in Cor. 2, which means larger models tend to benefit more from pre-training. With pre-trained knowledge preserved, AdapterGNN reduces the size of the tunable parameter space leading to less test error and thus superior generalization ability. Therefore, the best approach is pre-training on a larger model and utilizing delta tuning with fewer parameters.

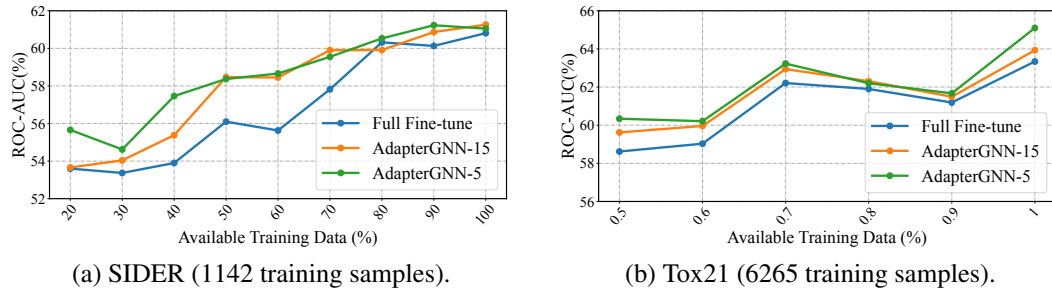


Figure 4: Test ROC-AUC (%) performances with different training data sizes.

Training data size. When the model size is fixed, reducing the size of the training samples results in inferior generalization ability, while AdapterGNN can mitigate this overfitting issue. To validate

Table 4: Comparison of different insertion forms.

Form	Position	Avg.
Full Fine-tune		69.6
Parallel	Before MP	70.4
Parallel	After MP	70.3
Parallel	Combine	71.2
Sequential	After MLP	70.2

Table 5: Comparison of learnable scaling and fixed scaling.

	BACE	BBBP	ClinTox	SIDER	Tox21	ToxCast	Avg.
0.01	77.8	67.6	76.3	59.9	74.8	62.5	69.8
0.05	78.2	68.8	77.8	61.2	76.2	63.2	70.9
0.1	78.5	67.6	72.6	61.0	76.2	63.3	69.9
0.5	78.7	67.6	72.3	60.9	76.2	63.3	69.8
1	78.6	68.7	66.3	61.3	75.7	63.3	69.0
5	73.7	66.6	55.9	60.8	75.3	62.9	65.9
Learnable	79.7	67.5	78.3	61.3	76.6	63.6	71.2

this, we compare the performance of full fine-tuning with two AdapterGNN settings, with bottleneck dimensions of 15 (default) and 5, respectively. The results presented in Fig. 4 demonstrate that when data becomes scarce, the performance of AdapterGNN with fewer tunable parameters decreases slower and obtains superior results. And fewer parameters in AdapterGNN yield better results.

Bottleneck dimension. Ablation study on the bottleneck dimension of AdapterGNN, as shown in Fig.5, demonstrates that reducing the bottleneck dimension to limit the size of tunable parameter space can improve the generalization ability of the model. But when the size is too small, the model may suffer from underfitting, which can restrict its performance. Therefore, selecting a bottleneck dimension of 15, which represents 5.2% of all parameters, yields the best average performance. Meanwhile, a dimension of 5, which accounts for only 2.2% of all parameters, can surpass the results of full fine-tuning.

Insertion form. AdapterGNN includes two adapters parallel to GNN MLP taking input before and after the message passing. To demonstrate the effectiveness of this design, we compare its performance with those of a single parallel adapter or a sequential adapter, which is inserted after GNN MLP. To ensure a fair comparison, we keep the count of adapter parameters the same across all forms. Our results in Table 4 show that adopting a single adapter alone already achieves superior performance over full fine-tuning. And combining two parallel adapters further improves the expressivity of delta tuning, yielding the best performance.

Scaling strategy. We compared our novel learnable scaling strategy with various fixed scaling ranging from 0.01 to 5. The results are presented in Table 5, with the highest performance in each dataset highlighted in bold. In five out of six datasets, as well as on average, our learnable scaling strategy achieved the highest performance. Meanwhile, among the fixed scalings, smaller scaling is superior, and a scaling factor of 0.05 achieved the highest performance. And as the scaling factor increased, the performance deteriorated due to catastrophic forgetting of pre-trained knowledge.

6 Conclusion

While many prompt-tuning methods have been proposed in GNNs, there is a gap between GNNs and transformers which makes prompt tuning less effective. Through comprehensive comparisons of delta tuning methods, we present a simple yet effective delta tuning framework for GNNs called AdapterGNN. This approach outperforms full fine-tuning with much fewer tunable parameters, improving both efficiency and effectiveness. We provide a theoretical justification for this improvement and find that our tasks fall within the classical regime of the generalization error, where a larger model can be worse, and reducing the size of the parameter space during tuning can result in lower test error. This explains the improved generalization ability and superior performance of AdapterGNN. One potential limitation is that we focus on the graph-level classification task on GINs and leave other tasks and GNN models for future exploration.

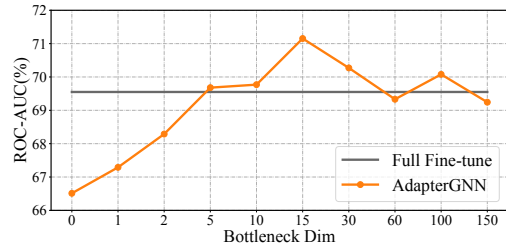


Figure 5: Performances with different bottleneck dimensions. 0 represents identical mapping.

References

- [1] Armen Aghajanyan, Luke Zettlemoyer, and Sonal Gupta. Intrinsic dimensionality explains the effectiveness of language model fine-tuning. *arXiv preprint arXiv:2012.13255*, 2020.
- [2] Sanjeev Arora, Rong Ge, Behnam Neyshabur, and Yi Zhang. Stronger generalization bounds for deep nets via a compression approach. In *International Conference on Machine Learning*, pages 254–263. PMLR, 2018.
- [3] Mikhail Belkin, Daniel Hsu, Siyuan Ma, and Soumik Mandal. Reconciling modern machine-learning practice and the classical bias–variance trade-off. *Proceedings of the National Academy of Sciences*, 116(32):15849–15854, 2019.
- [4] Tom Brown, Benjamin Mann, Nick Ryder, Melanie Subbiah, Jared D Kaplan, Prafulla Dhariwal, Arvind Neelakantan, Pranav Shyam, Girish Sastry, Amanda Askell, et al. Language models are few-shot learners. *Advances in neural information processing systems*, 33:1877–1901, 2020.
- [5] Shoufa Chen, Chongjian Ge, Zhan Tong, Jiangliu Wang, Yibing Song, Jue Wang, and Ping Luo. Adaptformer: Adapting vision transformers for scalable visual recognition. *arXiv preprint arXiv:2205.13535*, 2022.
- [6] Jacob Devlin, Ming-Wei Chang, Kenton Lee, and Kristina Toutanova. Bert: Pre-training of deep bidirectional transformers for language understanding. *arXiv preprint arXiv:1810.04805*, 2018.
- [7] Cameron Diao, Kaixiong Zhou, Xiao Huang, and Xia Hu. Molcpt: Molecule continuous prompt tuning to generalize molecular representation learning. *arXiv preprint arXiv:2212.10614*, 2022.
- [8] Ning Ding, Yujia Qin, Guang Yang, Fuchao Wei, Zonghan Yang, Yusheng Su, Shengding Hu, Yulin Chen, Chi-Min Chan, Weize Chen, et al. Delta tuning: A comprehensive study of parameter efficient methods for pre-trained language models. *arXiv preprint arXiv:2203.06904*, 2022.
- [9] Taoran Fang, Yunchao Zhang, Yang Yang, and Chunping Wang. Prompt tuning for graph neural networks. *arXiv preprint arXiv:2209.15240*, 2022.
- [10] Matthias Fey and Jan E. Lenssen. Fast graph representation learning with PyTorch Geometric. In *ICLR Workshop on Representation Learning on Graphs and Manifolds*, 2019.
- [11] Will Hamilton, Zhitao Ying, and Jure Leskovec. Inductive representation learning on large graphs. *Advances in neural information processing systems*, 30, 2017.
- [12] Xu Han, Zhengyan Zhang, Ning Ding, Yuxian Gu, Xiao Liu, Yuqi Huo, Jiezhong Qiu, Yuan Yao, Ao Zhang, Liang Zhang, et al. Pre-trained models: Past, present and future. *AI Open*, 2:225–250, 2021.
- [13] Moritz Hardt, Ben Recht, and Yoram Singer. Train faster, generalize better: Stability of stochastic gradient descent. In *International conference on machine learning*, pages 1225–1234. PMLR, 2016.
- [14] Junxian He, Chunting Zhou, Xuezhe Ma, Taylor Berg-Kirkpatrick, and Graham Neubig. Towards a unified view of parameter-efficient transfer learning. *arXiv preprint arXiv:2110.04366*, 2021.
- [15] Neil Houlsby, Andrei Giurgiu, Stanislaw Jastrzebski, Bruna Morrone, Quentin De Laroussilhe, Andrea Gesmundo, Mona Attariyan, and Sylvain Gelly. Parameter-efficient transfer learning for nlp. In *International Conference on Machine Learning*, pages 2790–2799. PMLR, 2019.
- [16] Edward J Hu, Yelong Shen, Phillip Wallis, Zeyuan Allen-Zhu, Yuanzhi Li, Shean Wang, Lu Wang, and Weizhu Chen. Lora: Low-rank adaptation of large language models. *arXiv preprint arXiv:2106.09685*, 2021.
- [17] Weihua Hu, Bowen Liu, Joseph Gomes, Marinka Zitnik, Percy Liang, Vijay Pande, and Jure Leskovec. Strategies for pre-training graph neural networks. *arXiv preprint arXiv:1905.12265*, 2019.
- [18] James Kirkpatrick, Razvan Pascanu, Neil Rabinowitz, Joel Veness, Guillaume Desjardins, Andrei A Rusu, Kieran Milan, John Quan, Tiago Ramalho, Agnieszka Grabska-Barwinska, et al. Overcoming catastrophic forgetting in neural networks. *Proceedings of the national academy of sciences*, 114(13):3521–3526, 2017.
- [19] Max Kuhn, Kjell Johnson, Max Kuhn, and Kjell Johnson. Over-fitting and model tuning. *Applied predictive modeling*, pages 61–92, 2013.
- [20] Yann LeCun, Yoshua Bengio, and Geoffrey Hinton. Deep learning. *nature*, 521(7553):436–444, 2015.

[21] Brian Lester, Rami Al-Rfou, and Noah Constant. The power of scale for parameter-efficient prompt tuning. *arXiv preprint arXiv:2104.08691*, 2021.

[22] Xiang Lisa Li and Percy Liang. Prefix-tuning: Optimizing continuous prompts for generation. *arXiv preprint arXiv:2101.00190*, 2021.

[23] Haokun Liu, Derek Tam, Mohammed Muqeeth, Jay Mohta, Tenghao Huang, Mohit Bansal, and Colin Raffel. Few-shot parameter-efficient fine-tuning is better and cheaper than in-context learning. *arXiv preprint arXiv:2205.05638*, 2022.

[24] Zemin Liu, Xingtong Yu, Yuan Fang, and Xinming Zhang. Graphprompt: Unifying pre-training and downstream tasks for graph neural networks. *arXiv preprint arXiv:2302.08043*, 2023.

[25] Mehryar Mohri, Afshin Rostamizadeh, and Ameet Talwalkar. *Foundations of machine learning*. MIT press, 2018.

[26] Wenlong Mou, Liwei Wang, Xiyu Zhai, and Kai Zheng. Generalization bounds of sgld for non-convex learning: Two theoretical viewpoints. In *Conference on Learning Theory*, pages 605–638. PMLR, 2018.

[27] Preetum Nakkiran, Gal Kaplun, Yamini Bansal, Tristan Yang, Boaz Barak, and Ilya Sutskever. Deep double descent: Where bigger models and more data hurt. *Journal of Statistical Mechanics: Theory and Experiment*, 2021(12):124003, 2021.

[28] Alex Yuxuan Peng, Yun Sing Koh, Patricia Riddle, and Bernhard Pfahringer. Using supervised pretraining to improve generalization of neural networks on binary classification problems. In *Machine Learning and Knowledge Discovery in Databases: European Conference, ECML PKDD 2018, Dublin, Ireland, September 10–14, 2018, Proceedings, Part I* 18, pages 410–425. Springer, 2019.

[29] Franco Scarselli, Marco Gori, Ah Chung Tsoi, Markus Hagenbuchner, and Gabriele Monfardini. The graph neural network model. *IEEE transactions on neural networks*, 20(1):61–80, 2008.

[30] Shai Shalev-Shwartz and Shai Ben-David. *Understanding machine learning: From theory to algorithms*. Cambridge university press, 2014.

[31] Teague Sterling and John J Irwin. Zinc 15–ligand discovery for everyone. *Journal of chemical information and modeling*, 55(11):2324–2337, 2015.

[32] Mingchen Sun, Kaixiong Zhou, Xin He, Ying Wang, and Xin Wang. Gppt: Graph pre-training and prompt tuning to generalize graph neural networks. In *Proceedings of the 28th ACM SIGKDD Conference on Knowledge Discovery and Data Mining*, pages 1717–1727, 2022.

[33] Shizhao Sun, Wei Chen, Liwei Wang, Xiaoguang Liu, and Tie-Yan Liu. On the depth of deep neural networks: A theoretical view. In *Proceedings of the AAAI Conference on Artificial Intelligence*, volume 30, 2016.

[34] Petar Velickovic, Guillem Cucurull, Arantxa Casanova, Adriana Romero, Pietro Lio, Yoshua Bengio, et al. Graph attention networks. *stat*, 1050(20):10–48550, 2017.

[35] Petar Velickovic, William Fedus, William L Hamilton, Pietro Lio, Yoshua Bengio, and R Devon Hjelm. Deep graph infomax. *ICLR (Poster)*, 2(3):4, 2019.

[36] Zhengyang Wang, Meng Liu, Youzhi Luo, Zhao Xu, Yaochen Xie, Limei Wang, Lei Cai, Qi Qi, Zhuoning Yuan, Tianbao Yang, et al. Advanced graph and sequence neural networks for molecular property prediction and drug discovery. *Bioinformatics*, 38(9):2579–2586, 2022.

[37] Jason Wei, Yi Tay, Rishi Bommasani, Colin Raffel, Barret Zoph, Sebastian Borgeaud, Dani Yogatama, Maarten Bosma, Denny Zhou, Donald Metzler, et al. Emergent abilities of large language models. *arXiv preprint arXiv:2206.07682*, 2022.

[38] Xuansheng Wu, Kaixiong Zhou, Mingchen Sun, Xin Wang, and Ninghao Liu. A survey of graph prompting methods: Techniques, applications, and challenges. *arXiv preprint arXiv:2303.07275*, 2023.

[39] Zonghan Wu, Shirui Pan, Fengwen Chen, Guodong Long, Chengqi Zhang, and S Yu Philip. A comprehensive survey on graph neural networks. *IEEE transactions on neural networks and learning systems*, 32(1):4–24, 2020.

[40] Jun Xia, Lirong Wu, Jintao Chen, Bozhen Hu, and Stan Z Li. Simgrace: A simple framework for graph contrastive learning without data augmentation. In *Proceedings of the ACM Web Conference 2022*, pages 1070–1079, 2022.

- [41] Jun Xia, Yanqiao Zhu, Yuanqi Du, and Stan Z Li. A survey of pretraining on graphs: Taxonomy, methods, and applications. *arXiv preprint arXiv:2202.07893*, 2022.
- [42] Keyulu Xu, Weihua Hu, Jure Leskovec, and Stefanie Jegelka. How powerful are graph neural networks? *arXiv preprint arXiv:1810.00826*, 2018.
- [43] Yuning You, Tianlong Chen, Yongduo Sui, Ting Chen, Zhangyang Wang, and Yang Shen. Graph contrastive learning with augmentations. *Advances in neural information processing systems*, 33:5812–5823, 2020.
- [44] Elad Ben Zaken, Shauli Ravfogel, and Yoav Goldberg. Bitfit: Simple parameter-efficient fine-tuning for transformer-based masked language-models. *arXiv preprint arXiv:2106.10199*, 2021.
- [45] Chiyuan Zhang, Samy Bengio, Moritz Hardt, Benjamin Recht, and Oriol Vinyals. Understanding deep learning (still) requires rethinking generalization. *Communications of the ACM*, 64(3):107–115, 2021.
- [46] Fan Zhou, Chengtai Cao, Kunpeng Zhang, Goce Trajcevski, Ting Zhong, and Ji Geng. Meta-gnn: On few-shot node classification in graph meta-learning. In *Proceedings of the 28th ACM International Conference on Information and Knowledge Management*, pages 2357–2360, 2019.
- [47] Kaixiong Zhou, Qingquan Song, Xiao Huang, and Xia Hu. Auto-gnn: Neural architecture search of graph neural networks. *arXiv preprint arXiv:1909.03184*, 2019.

A Preliminaries

Our paper focuses on the graph-level classification task. Let tuple $\mathcal{G} = (\mathcal{V}, \mathcal{E}, \mathbf{X}_{\mathcal{V}}, \mathbf{X}_{\mathcal{E}}) \in \mathbb{G}$ denotes a graph from a dataset \mathbb{G} , where $\mathcal{V} = \{v_1, v_2, \dots, v_N\}$ and \mathcal{E} are sets of nodes and edges. The adjacency matrix is $\mathbf{A} \in \{0, 1\}^{N \times N}$, where $\mathbf{A}_{ij} = 1$ represents $(v_i, v_j) \in \mathcal{E}$. $\mathbf{X}_{\mathcal{V}} \in \mathbb{R}^{N \times \mathbb{F}_{\mathcal{V}}}$ is the node feature matrix, where $x_i \in \mathbb{R}^{\mathbb{F}_{\mathcal{V}}}$ is the feature of the node v_i . $\mathbf{X}_{\mathcal{E}} \in \mathbb{R}^{M \times \mathbb{F}_{\mathcal{E}}}$ is the edge feature matrix, where $x_{ij} \in \mathbb{R}^{\mathbb{F}_{\mathcal{E}}}$ is the feature of the edge (v_i, v_j) . These feature matrices are optional.

Graph-level Classification Task. A GNN encoder is often represented as f_{θ} and encodes a graph as $h = f_{\theta}(\mathcal{G})$, where h is the feature embedding of the input graph \mathcal{G} and θ is parameters of the encoder. Then a classifier g_{ϕ} takes h as input and gives classification probability $\hat{y} = g_{\phi}(h) \in \mathbb{R}^C$, where C is the number of classes and ϕ is the parameters of the classifier. The predicted output is $\text{argmax}(\hat{y})$. And for training, the target loss function is $\mathcal{L}(y, \hat{y})$, where y is the ground truth label for \mathcal{G} .

Pre-training and Fine-tuning GNN Models. The pre-training procedure aims to give a superior initialization of θ , as θ_S . It always utilizes larger datasets \mathbb{G}_S . Here we give the formulation under a supervised manner to pre-train f_{θ} as an example:

$$\min_{\theta, \phi} \sum_{(\mathcal{G}_i, y_i) \in \mathbb{G}_S} \mathcal{L}^S(g_{\phi}(f_{\theta}(\mathcal{G}_i)), y_i). \quad (9)$$

where the optimized θ is the pre-trained output θ_{pre} . Note that many unsupervised manners [17] are also applicable and the formulation can be diverse.

The pre-trained GNN encoder is task-agnostic and can be transferred to different downstream tasks. However, the classifier is task-specific, so it is not retained. The fine-tuning task is always supervised, allowing us to use the following formulation:

$$\begin{aligned} \min_{\theta, \phi} & \sum_{(\mathcal{G}_i, y_i) \in \mathbb{G}_T} \mathcal{L}^T(g_{\phi}(f_{\theta}(\mathcal{G}_i)), y_i), \\ \text{s.t. } & \theta_{init} = \theta_S. \end{aligned} \quad (10)$$

Delta tuning GNN Models. Delta tuning is a technique that, similar to fine-tuning, makes use of the pre-trained encoder θ_S . However, during the tuning stage, delta tuning differs from fine-tuning in that it only updates part of θ [44] or inserts additional modules to θ and updates only the inserted

modules [15; 22; 16; 21]. In the context of GNNs, these parameters can be represented as ψ , and they are updated in conjunction with the classifier:

$$\min_{\psi, \phi} \sum_{(\mathcal{G}_i, y_i) \in \mathbb{G}_T} \mathcal{L}^T(g_\phi(f_{\theta_S, \psi}(\mathcal{G}_i)), y_i). \quad (11)$$

where $f_{\theta_S, \psi}$ is the modified encoder and the original parameters θ_S (or most of them) are fixed during delta tuning. Delta tuning is more efficient and the tunable parameter space is much smaller than the original: $|\psi| \ll |\theta|$.

B Detailed Derivations

B.1 Detailed Proof for Generalization Bounds for Finite Hypothesis Space in Classical Regime

Let \mathcal{H} be a finite hypothesis space, $h \in \mathcal{H}$ is a group of trained parameters within parameter space \mathcal{H} . $\hat{\mathcal{E}}_{\mathcal{D}_n}$ represents training error over sampled training data \mathcal{D}_n , and \mathcal{E} represents test error. n is the number of training data.

We begin by analyzing the probability δ that the test error for a hypothesis space h will surpass the training error by a value greater than ε :

$$\delta = P\left(\exists h \in \mathcal{H}, \left|\hat{\mathcal{E}}_{\mathcal{D}_n}(h) - \mathcal{E}(h)\right| \geq \varepsilon\right). \quad (12)$$

From the theorem of the union bound of probability, we can get:

$$\begin{aligned} \delta &= P\left(\exists h \in \mathcal{H}, \left|\hat{\mathcal{E}}_{\mathcal{D}_n}(h) - \mathcal{E}(h)\right| \geq \varepsilon\right) \\ &= P\left(\left[\left|\hat{\mathcal{E}}_{\mathcal{D}_n}(h_1) - \mathcal{E}(h_1)\right| \geq \varepsilon\right] \vee \dots \vee \left[\left|\hat{\mathcal{E}}_{\mathcal{D}_n}(h_{|\mathcal{H}|}) - \mathcal{E}(h_{|\mathcal{H}|})\right| \geq \varepsilon\right]\right) \\ &\leq \sum_{h \in \mathcal{H}} P\left(\left|\hat{\mathcal{E}}_{\mathcal{D}_n}(h) - \mathcal{E}(h)\right| \geq \varepsilon\right). \end{aligned} \quad (13)$$

Then we refer to Hoeffding's Inequality:

Theorem 2 Hoeffding's Inequality: Let $\{X_i\} = \{X_1, X_2, \dots, X_n\}$ be independent random variables such that $a_i \leq X_i \leq b_i$ almost surely. The following inequality holds:

$$P\left(\left|\sum_{i=1}^n (X_i - \mathbb{E}X_i)\right| \geq \varepsilon\right) \leq 2 \exp\left[-\frac{2\varepsilon^2}{\sum_{i=1}^n (b_i - a_i)^2}\right]. \quad (14)$$

We define our training error as $X_i = \ell(h(\mathbf{x}_i), y_i)$ for $(\mathbf{x}_i, y_i) \in \mathcal{D}_n$. Thus the test error is the expectation of X_i . We can give:

$$\begin{aligned} \sum_{i=1}^n (X_i - \mathbb{E}X_i) &= n \left\{ \left[\frac{1}{n} \sum_{i=1}^n \ell(h(\mathbf{x}_i), y_i) \right] - \mathbb{E}_{(\mathbf{x}, y) \sim D} \ell(h(\mathbf{x}), y) \right\} \\ &= n \left(\hat{\mathcal{E}}_{\mathcal{D}_n}(h) - \mathcal{E}(h) \right). \end{aligned} \quad (15)$$

Meanwhile, we assume that 01-loss is adopted as $\ell(h(\mathbf{x}_i), y_i) \in [0, 1] = [a_i, b_i]$. Therefore, taking the above conditions into Eq. 14, we obtain:

$$P\left(n \left| \hat{\mathcal{E}}_{\mathcal{D}_n}(h) - \mathcal{E}(h) \right| \geq \varepsilon\right) \leq 2e^{-\frac{2\varepsilon^2}{n}}. \quad (16)$$

Taking it back to Eq. 13:

$$\delta \leq 2|\mathcal{H}| \exp(-2n\varepsilon^2). \quad (17)$$

$$\log \frac{\delta}{2} \leq \log |\mathcal{H}| - 2n\epsilon^2. \quad (18)$$

$$\epsilon \leq \sqrt{\frac{\log |\mathcal{H}| - \log \frac{\delta}{2}}{2n}}. \quad (19)$$

Note that Eq. 12 is eqivelant to:

$$1 - \delta = P \left(\forall h \in \mathcal{H}, \left| \hat{\mathcal{E}}_{\mathcal{D}_n}(h) - \mathcal{E}(h) \right| < \epsilon \right). \quad (20)$$

Finally, we have:

$$P \left(\forall h \in \mathcal{H}, \left| \hat{\mathcal{E}}_{\mathcal{D}_n}(h) - \mathcal{E}(h) \right| \leq \sqrt{\frac{\log |\mathcal{H}| - \log \frac{\delta}{2}}{2n}} \right) \geq 1 - \delta. \quad (21)$$

Therefore, with probability at least $1 - \delta$:

$$\forall h \in \mathcal{H}, \quad \mathcal{E}(h) \leq \hat{\mathcal{E}}_{\mathcal{D}_n}(h) + O \left(\sqrt{\frac{\log |\mathcal{H}| + \log \frac{2}{\delta}}{2n}} \right). \quad (22)$$

The theorem states that the test error is statistically bounded by three factors: the training error $\hat{\mathcal{E}}$, the size of the hypothesis space $\log |\mathcal{H}|$, and the number of training samples n .

For simplicity, we omit the probability notation and use \mathcal{U} to represent the upper bound. We will also omit the log term and use \mathcal{P} to represent the parameter space. Therefore, $|\mathcal{P}|$ will quantify the size of the parameter space. Sampled data \mathcal{D}_n and the trained parameters \mathcal{P} are variables of training error $\hat{\mathcal{E}}$:

$$\mathcal{E} \leq \mathcal{U}(\mathcal{E}) = \hat{\mathcal{E}}(\mathcal{D}_n, \mathcal{P}) + O \left(\sqrt{|\mathcal{P}|/n} \right). \quad (23)$$

B.2 Detailed Proof for Corallary 1

For the upper bound of the task: $\mathcal{U}(\mathcal{E}_T) = \hat{\mathcal{E}}(\mathcal{D}_{n_T}^T, \mathcal{P}_T) + O \left(\sqrt{|\mathcal{P}_T|/n_T} \right)$. First, we can infer that With the increase of $|\mathcal{P}_T|$, a larger parameter size confers stronger optimization ability, leading to the decrease of the first term training error $\hat{\mathcal{E}}(\mathcal{D}_{n_T}^T, \mathcal{P}_T)$.

Meanwhile, the second term generalization gap bounds $O \left(\sqrt{|\mathcal{P}_T|/n_T} \right)$ increases.

We can get the partial derivative of $\mathcal{U}(\mathcal{E}_T)$ along with $|\mathcal{P}_T|$:

$$\frac{\partial(\mathcal{U}(\mathcal{E}_T))}{\partial |\mathcal{P}_T|} = \frac{\partial(\hat{\mathcal{E}}(\mathcal{D}_{n_T}^T, \mathcal{P}_T))}{\partial |\mathcal{P}_T|} + \frac{\partial O \left(\sqrt{|\mathcal{P}_T|/n_T} \right)}{\partial |\mathcal{P}_T|} = \frac{\partial(\hat{\mathcal{E}}(\mathcal{D}_{n_T}^T, \mathcal{P}_T))}{\partial |\mathcal{P}_T|} + O(1/\sqrt{|\mathcal{P}_T| \cdot n_T}). \quad (24)$$

The first term $\frac{\partial(\hat{\mathcal{E}}(\mathcal{D}_{n_T}^T, \mathcal{P}_T))}{\partial |\mathcal{P}_T|} < 0$ and the second term $O(1/\sqrt{|\mathcal{P}_T| \cdot n_T}) > 0$.

Empirically, we have observed that when the size of parameter space, denoted by $|\mathcal{P}_T|$, is extremely large, the risk of overfitting is high, leading to a large test error $\mathcal{U}(\mathcal{E}_T)$. Conversely, when $|\mathcal{P}_T|$ is extremely small, the model may not be able to fit the data well, again resulting in a large test error $\mathcal{U}(\mathcal{E}_T)$.

Therefore, there exists an extreme point where the partial derivative of $\mathcal{U}(\mathcal{E}_T)$ with respect to $|\mathcal{P}_T|$ is zero, and this point corresponds to a minimum. Given a fixed n_T and $\mathcal{D}_{n_T}^T$, we can choose the optimal value of $|\bar{\mathcal{P}}_T|$ to minimize the test error $\mathcal{U}(\mathcal{E}_T)$, where $\partial(\hat{\mathcal{E}}(\mathcal{D}_{n_T}^T, \bar{\mathcal{P}}_T))/\partial |\mathcal{P}_T| + O(1/\sqrt{|\mathcal{P}_T| \cdot n_T}) = 0$.

B.3 Detailed Proof for Corollary 2

Data for the pre-training task S is more abundant than downstream task T , satisfying $n_S > n_T$. For task S , we have the generalization upper bounds as: $\mathcal{U}(\mathcal{E}_S) = \hat{\mathcal{E}}(\mathcal{D}_{n_S}^S, \mathcal{P}_S) + O\left(\sqrt{|\mathcal{P}_S|/n_S}\right)$.

From Coll.1, we have known that:

$$\frac{\partial(\mathcal{U}(\mathcal{E}_T))}{\partial|\mathcal{P}|} \Big|_{|\mathcal{P}|=|\bar{\mathcal{P}}_T|} = \frac{\partial(\hat{\mathcal{E}}(\mathcal{D}_{n_T}^T, \bar{\mathcal{P}}_T))}{\partial|\mathcal{P}|} + O(1/\sqrt{|\bar{\mathcal{P}}_T| \cdot n_T}) = 0. \quad (25)$$

Practically, we often leverage data from the same source to pre-train. For example, unlabeled molecular graphs are used to pre-train and the labeled ones are for fine-tuning in our experiments. The property of data is similar: $\hat{\mathcal{E}}(\mathcal{D}_{n_T}^T, \mathcal{P}) \approx \hat{\mathcal{E}}(\mathcal{D}_{n_S}^S, \mathcal{P})$

Considering $n_S > n_T$ and $O(1/\sqrt{|\bar{\mathcal{P}}_T| \cdot n_T}) > 0$, we can obtain the following inequality:

$$\frac{\partial(\mathcal{U}(\mathcal{E}_S))}{\partial|\mathcal{P}|} \Big|_{|\mathcal{P}|=|\bar{\mathcal{P}}_T|} = \frac{\partial(\hat{\mathcal{E}}(\mathcal{D}_{n_S}^S, \bar{\mathcal{P}}_T))}{\partial|\mathcal{P}|} + O(1/\sqrt{|\bar{\mathcal{P}}_T| \cdot n_S}) < 0. \quad (26)$$

Meanwhile, for S , we have the optimal $|\bar{\mathcal{P}}_S|$ to get:

$$\frac{\partial(\mathcal{U}(\mathcal{E}_S))}{\partial|\mathcal{P}|} \Big|_{|\mathcal{P}|=|\bar{\mathcal{P}}_S|} = \frac{\partial(\hat{\mathcal{E}}(\mathcal{D}_{n_S}^S, \bar{\mathcal{P}}_S))}{\partial|\mathcal{P}|} + O(1/\sqrt{|\bar{\mathcal{P}}_S| \cdot n_S}) = 0. \quad (27)$$

Combining the above two formulas and recall $|\bar{\mathcal{P}}_S|$ is the minimum point:

$$\frac{\frac{\partial(\mathcal{U}(\mathcal{E}_S))}{\partial|\mathcal{P}|} \Big|_{|\mathcal{P}|=|\bar{\mathcal{P}}_T|}}{\frac{\partial(\mathcal{U}(\mathcal{E}_S))}{\partial|\mathcal{P}|} \Big|_{|\mathcal{P}|=|\bar{\mathcal{P}}_S|}} > \frac{\mathcal{U}(\mathcal{E}_S) \Big|_{|\mathcal{P}|=|\bar{\mathcal{P}}_T|}}{\mathcal{U}(\mathcal{E}_S) \Big|_{|\mathcal{P}|=|\bar{\mathcal{P}}_S|}} \quad (28)$$

From this, we get $|\bar{\mathcal{P}}_S| > |\bar{\mathcal{P}}_T|$.

C Extended Analysis

C.1 Analysis of the Relationship Between GNN Size and Error

Here, by analyzing the relationship between GNN size and test/training error, we empirically show our tasks fall within the scope of the classical regime of generalization theory, where the test error follows the U-shaped behavior, i.e., decreases and then increases as the model size grows. From this, we can infer the satisfaction of Ineq. 5 in our experiments of GNNs: $\hat{\mathcal{E}}(\mathcal{D}_{n_T}^T, \bar{\mathcal{P}}_S) + O\left(\sqrt{|\bar{\mathcal{P}}_S|/n_T}\right) > \hat{\mathcal{E}}(\mathcal{D}_{n_T}^T, \bar{\mathcal{P}}_T) + O\left(\sqrt{|\bar{\mathcal{P}}_T|/n_T}\right)$, where $|\bar{\mathcal{P}}_S| > |\bar{\mathcal{P}}_T|$. This inequality suggests that smaller model sizes typically lead to lower test errors when training a model from scratch. This forms the basis for the effectiveness of our delta tuning method.

We conducted experiments on six small molecular datasets, varying model sizes in two ways: (1) by varying embedding dimensions while fixing the MLP middle dimension at twice the embedding dimensions, and (2) by fixing embedding dimensions at 300 and varying the middle dimensions. The results are presented in Figures 6 and 7. For all datasets, we made two observations. First, the test error initially decreases and then increases as the model size grows. Second, the training error does not approach zero, indicating that even a large model is not over-parameterized [27]. These observations suggest that our tasks fall within the scope of the classical regime and reducing the size of the parameter space, unless too small, can help improve generalization ability.

It is important to note that the phenomenon in question occurs exclusively in the context of training from scratch. To leverage the knowledge gained from pre-training, employing a larger model is necessary. To enhance the generalization ability of this large model, the full fine-tuning approach can

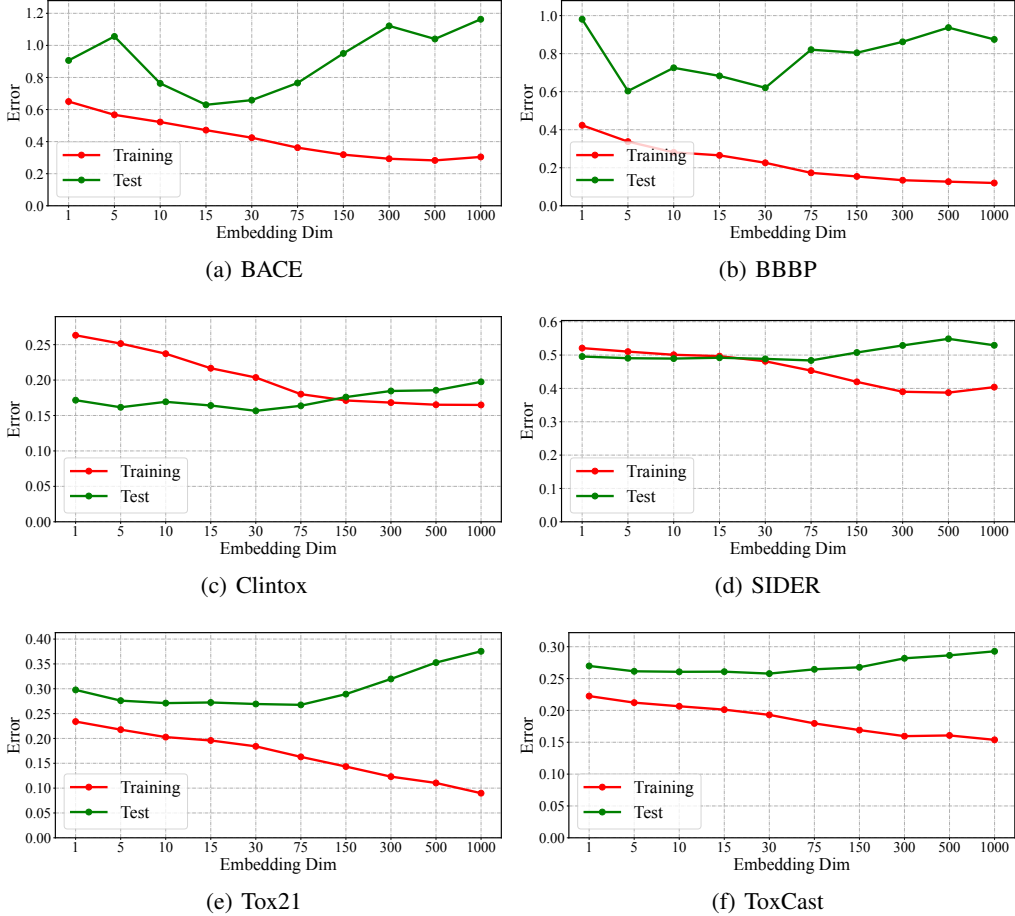


Figure 6: Without pre-training, the training and test error across different model sizes, measured by GNN MLP embedding dimensions.

be replaced with delta tuning. As illustrated in Fig. 3(a), embedding dimensions between 200 to 300 exhibit the highest performance for full fine-tuning, albeit with inferior test error when training from scratch. Our AdapterGNN outperforms full fine-tuning consistently, implying that pre-training on a larger model and utilizing delta tuning with fewer parameters is the optimal approach.

D Experiment Details

D.1 Implementations of AdapterGNN

PyTorch and PyG [10] are used to conduct all experiments on NVIDIA A100 GPUs in this work. All hyperparameters and training strategies are consistent with the previous work [17]. The data is split into the out-of-distribution scaffold and species splits, which are also consistent. For full fine-tuning, the default embedding dimension is set to 300. For the AdapterGNN hyperparameters, the bottleneck dimension is set to 15, and the starting value of the learnable scaling is set to 0.01. Our results are achieved **WITHOUT** any special hyperparameter tuning for individual datasets to ensure efficiency. In practice, we also tune the bias of the original MLPs as BitFit [44]. It keeps efficiency and can provide additional improvement.

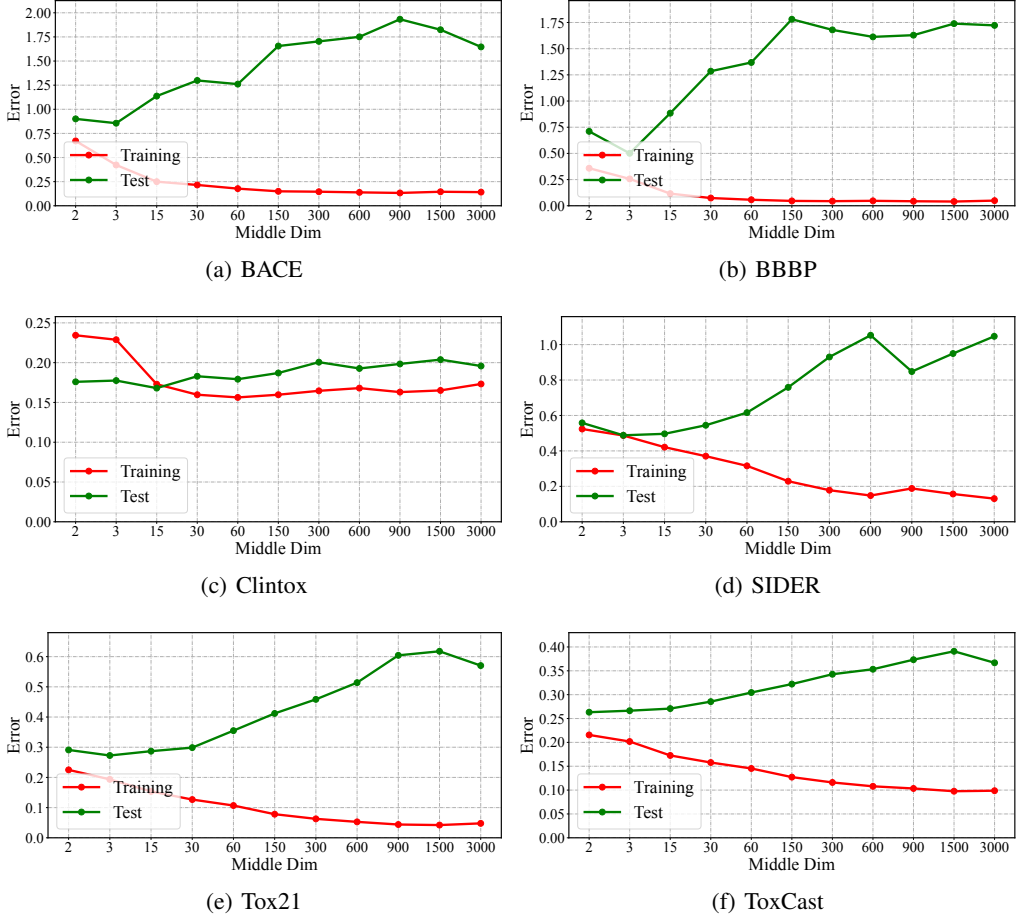


Figure 7: Without pre-training, the training and test error across different model sizes, measured by GNN MLP middle dimensions.

D.2 Implementation Details of Other Delta Tuning Techniques in GNNs

Recently, researchers have proposed several delta tuning methods. However, most of them are only applied to the transformer-based model in the NLP field. Here, we will detail how we utilize these methods in GNNs.

Frozen. We use this method as our baseline. In experiments, we have discovered that learnable affine parameters for batch normalization are crucial for achieving stable performance. Therefore, we have fine-tuned these parameters for all delta tuning methods. These parameters are the only ones that can be adjusted for the frozen baseline and they only occupy 0.16% of all parameters.

BitFit [44]. We tune all bias parameters of each linear layer in each GNN MLP. This technique brings slight improvement in performance.

(IA)³ [23]. In each GNN MLP, we modify the input of the linear layer by incorporating learnable weights. Specifically, if the embedding dimension is denoted as n_{ebd} , then the input to the linear layer is of shape $n_{batch} \times n_{ebd}$. We design learnable weights of shape n_{ebd} and reweight the input by element-wise multiplication with these weights before feeding it into the linear layer. This approach is both efficient and effective. However, due to the limited number of tunable parameters (only 0.24% of the total), the expressivity of the model is still restricted.

Table 6: Statistics of datasets for downstream tasks.

Dataset	BACE	BBBP	ClinTox	HIV	Sider	Tox21	MUV	ToxCast	PPI
# Graphs	1513	2039	1478	41127	1427	7831	93087	8575	88k
# Tasks	1	1	2	1	27	12	17	617	40

LoRA [16]. LoRA modifies the output of the linear layer in each MLP. To achieve this, it uses a parallel module that consists of two sequential linear layers with a bottleneck dimension. The module takes the same input as the original linear layer and adds its output to the original output. By using a small bottleneck, the size of tunable parameters is reduced from $n_{in} \times n_{out}$ to $n_{in} \times n_{bottleneck} + n_{bottleneck} \times n_{out}$. Furthermore, after delta tuning, the tuned linear layers can be multiplied and directly added to the original frozen linear layer. This process results in no extra parameters during inference. Although LoRA achieves higher performance with more parameters, it is still no better than full fine-tuning.

Prompt. Prompt tuning is a widely acknowledged technique in the NLP field, which involves modifying the input of the network while keeping the parameters fixed. In GNNs, there are two types of prompt tuning techniques: feature prompt (feat) and node prompt (node). With the feature prompt, a learnable feature is added to the node embedding. In addition to previous work [9], we also tune batch normalization. For the node prompt, a fully connected learnable virtual node is added to each GNN layer. Prompt tuning is a highly efficient technique, but its performance in GNNs is not as good as in NLP. We conjecture that this is due to the gap between GNNs and transformer-based models. In GNNs, modifying the input alone may not achieve the same level of expressivity as in NLP [14], which could be one of the reasons for the performance gap.

Adapter [15]. Similar to LoRA, the adapter also utilizes two sequential linear layers with a bottleneck to add its output to the original output. Additionally, an activation layer is inserted to form an adapter, and an additional batch normalization layer is added behind it. We evaluate two types of adapters: sequential (seq) and parallel (par). The sequential adapter takes the output of each GNN layer as input and adds its output to the original GNN layer output in the end. The parallel adapter takes the input before GNN MLP (or before message passing) as input and adds its output to the original output of GNN MLP. Notably, this is also different from LoRA. The adapter is parallel to GNN MLP, while LoRA is parallel to the linear layer of GNN MLP. With these advanced techniques, the adapter has improved expressivity and achieves superior performance, even outperforming full fine-tuning with only 5% of the total parameters. Therefore, our AdapterGNN primarily adopts several techniques from adapters.

Partial. We have implemented a partial fine-tuning approach for our GNN layers. Specifically, Partial-1 indicates that only the last layer is fine-tuned, whereas Partial-3 indicates that the last three layers are fine-tuned. However, this technique is not quite efficient. And our experiments have shown that it only achieves a similar performance as full fine-tuning.

D.3 Details of Datasets

For pre-training, the dataset of the chemistry domain contains 2 million unlabeled molecules sampled from the ZINC15 [31] database. The dataset of the biology domain contains 395K unlabeled protein ego-networks from PPI networks.

For downstream fine-tuning, we utilize eight binary classification datasets published for downstream tasks in the chemistry domain. For the biology domain, we use 88K labeled protein ego-networks from PPI networks to form 40 binary classification tasks to predict fine-grained biological functions. These datasets are adopted in Hu.’s work [17]. We provide detailed statistics of our downstream datasets in Table 6. The first eight datasets pertain to the chemistry domain, while the last PPI dataset is related to the biology domain.

D.4 Details of Pre-trained GNN Models

To ensure a fair comparison, we conducted experiments following the same settings outlined in the previous work [17]. We utilized a 5-layer GIN backbone, open-source pre-trained checkpoints, and the same fine-tuning hyperparameters. We adopt six different pre-training strategies. Specifically, EdgePred [11] masks and reconstructs edges to predict edge existence. Infomax [35] trains a node encoder that maximizes the mutual information between local and global graph representation. Hu.’s work [17] proposes AttrMasking and ContextPred which can explore graph attributes and structure. GraphGL [43] proposes a graph contrastive learning framework for learning unsupervised representations of graph data. SimGRACE [40] takes the GNN model with its perturbed version as two encoders to obtain two correlated views for contrastive learning without data augmentations. For the latter two, we used the default checkpoints available in their published repositories without grid searching for fair and efficient comparison.